Analysis of two cancer models with a proposed therapy based on replicator dynamics

Maria Alejandra Sandoval

July 26, 2022

Abstract

This paper reviews a cancer model based on the evolutionary dynamics of population games. In particular, we analyze two models of cancer, to determine which one resembles reality the most, and with this one, propose a therapy based on replicator dynamics. We also perform a sensitivity analysis of the models to determine and compare specific changes. The sensitivity analysis of the parameters, as well as our proposal, are represented by numerical simulations. Finally, our proposed method generates therapy over time, depending on densities.

1 Introduction

Cancer arises when there are abnormalities in the cell reproduction process [1]. The scientists have developed many studies throughout history. In the beginning and until today, work continues on the biological aspects, understanding its formation, where they come from, and even the multiple genomes that affect it [2]. However, this has not been enough to be able to study it, so people had to resort evolutionary strategies and cancer ecology [3][4]. From this point, scientists understood that cancer has evolutionary principles and can analyze it from an eco-evolutionary point of view towards better outcomes or outright cure [5][6][7]. Cancer is studied from different aspects, and the following mind-map (Fig. 1) links the main aspects.

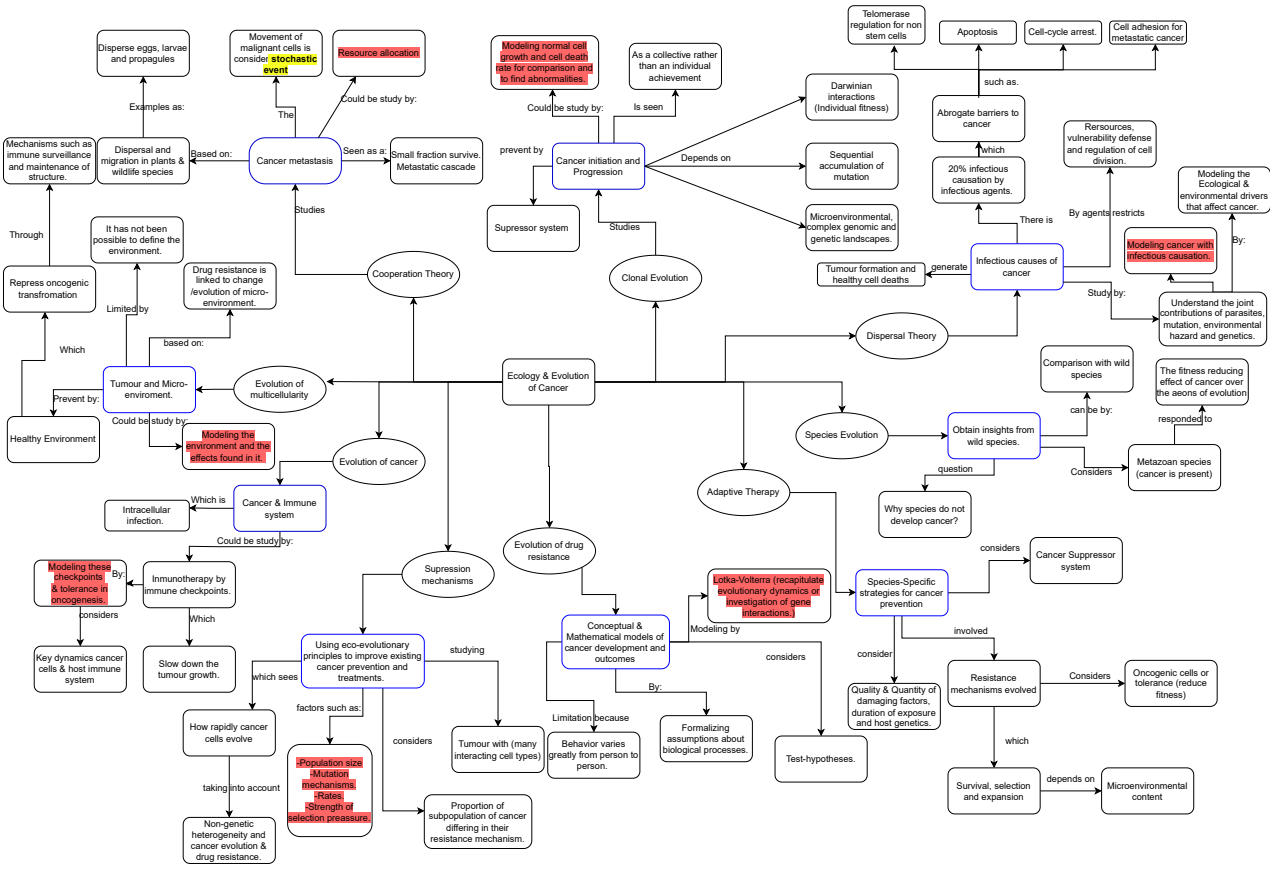

Figure 1: Mind map based on possible cancer studies, summary of [5].

There are many works developed around cancer and evolutionary dynamics. Some examples are the ones that study the dynamics between the three cells involved in the cancer process [8]; other works consider the cells' competitive effect after tumor removal [9][10] to even some developed relationships between extracellular matrices [11]. Some articles relate tumor growth by taking into account different strategies [12], the relationship among models to demonstrate such growths, predictive models [13], or represent therapy already applied [14].

Some works have included aspects of therapy to address these problems but in a time-invariant way. Considering how to model suppressor genes [15], or understanding how to use the contribution of evolutionary game theory for treatment [16]. Other works involve game dynamics such as the prisoner's dilemma [17] or Darwinian models involving certain environmental factors [18][19]. Many papers focus on modifying the payoff matrices as if populations interact as games to link them and apply a type of therapy [20]. Others analyze obstruction in the cooperation of the population [21][22][23]. All these studies model a process that has already occurred but do not consider how to control it.

Unlike the previous work, the goal of this paper is first, to identify a model, compare it, use it in a generalized way, and then generate control over the therapy applied to this cancer model. This paper addresses the aspect of the evolution of drug resistance seen in the mind map at the bottom of Fig.1. We consider two models; one relating the population of two types of cancer cells in tumor formation [24]; and another relating healthy cells and cancer cells [25]. We have considered and analyze both models to determine which one is more similar to real life based on scientific literature that explain a system input an output parameters. Also, considering what we have seen in [26], we perform dynamic therapies applied to our problem. Additionally, we take into account the different models that include population dynamics [27][28][29][30][31] applied to biology to show generalized dynamics. We apply the replicator dynamics [32] for therapy within population dynamics as opposed to [33] which applies it to the dynamics itself.

Consequently, the contribution of this paper is a theoretical analysis of two models, plus a replicator dynamics therapy for density dependence applied to the model that resembles reality.
The following is the organization of the paper. First, Section II states the problem statement of the model analysis and our final model. Next, Section III presents the two models and our proposed approach. Afterward, Section VI depicts the sensitivity analysis of the models, their comparison, and some numerical experiments to our approach. Finally, Section V concludes the paper.

2 Models and Problem Statement

2.1 Models

This paper considers two cancer models to perform a sensitivity analysis of the constants and compare them. Therefore, we determine which of these models to use to modify the therapy. The first model is taken from the paper [24], which describes the population dynamics between two types of cancer cells. The second model is taken from the paper [25], which describes the population dynamics between healthy cells and cancer cells. The main goal is to analyze the constants in each model to determine which model, according to scientific literature, approximates better actual environment conditions and to specify why. For both models, we review the behavior of the state variables through time. Then, for the one chosen, we review the behavior of the phase diagrams including equilibrium points between two state variables.

To define both models, we use the definition of variables and parameters in each paper. We have not defined a unified notation for both papers because there are different parameters in each one. In [24] they relate two types of cancer cells and in [25] there are both, healthy and cancer cells. In [24] there are three cases. For the first case there are four variables, let x_i, where $i \in \{1, 2\}$ the type of cancer cells population. Also, $x(t) = x_1(t) + x_2(t)$ is the tumor size and $g = \frac{x_1(t)}{x(t)}$ is the tumor composition. For the parameters of the model, there are K which is the carrying capacity, T the Allee-threshold, c_i the cell death rates $i \in \{1, 2\}$, m_i the mutation rates, and α the convexity parameter. For the second case, they include the variable $\gamma_i(t)$, which represents the therapy and adds to the cell death rates. The third case includes μ_i, representing the mutation therapy and adding to the mutation rates. Finally the payoff matrix used in these three cases, is defined as $A_{11} = r_1$, $A_{12} = d_1$, $A_{21} = r_2$ and $A_{22} = d_2$, where r_i represents the growth of population i and d_i represents the effect of the other population with respect to population i.

For the second model, there are four variables. Let y_i represent cells population, where $y_1(t)$ are healthy cells and $y_2(t)$ are cancer cells. Let $u_i(t)$ represent the strategies, where $i \in \{1, 2\}$, and $v = u_i$ for each cell population. Now r represents the intrinsic growth rate to all cells, $K(v)$ is carrying capacity, and $\alpha(v, u_j)$ determines the competitive effect of using different strategies. They use parameters such as σ_k^2 and σ_α^2 which are variances in the distribution functions. Also, they use σ_1^2 and σ_2^2 representing evolution of each cell. Finally, for this model, there is a parameter k_m which represents the maximum of the carrying capacity and β which varies the distribution.

2.1.1 Model in [24]

This model includes 3 cases; the first case is about the tumor growth, the second case is about tumor growth with cytotoxic therapy, and the third case includes mutation therapy.
Tumor growth

$$\dot{x}_1 = x_1(r_1 g^\alpha + d_1(1-g)^\alpha)\left(\frac{x}{T} - 1\right)\left(1 - \frac{x}{K}\right) - c_1 x_1 - m_1 x_1 + m_2 x_2, \tag{1}$$

$$\dot{x}_2 = x_2(r_2(1-g)^\alpha + d_2 g^\alpha)\left(\frac{x}{T} - 1\right)\left(1 - \frac{x}{K}\right) - c_2 x_2 - m_2 x_2 + m_1 x_1. \tag{2}$$

Or seen as:

$$\dot{x} = gx(r_1 g^\alpha + d_1(1-g)^\alpha)\left(\frac{x}{T}-1\right)\left(1-\frac{x}{K}\right) - c_1 gx + (x-gx)(r_2(1-g)^\alpha + d_2 g^\alpha)\left(\frac{x}{T}-1\right)\left(1-\frac{x}{K}\right) - c_2(x-gx)$$
$$\dot{g} = g(r_1 g^\alpha + d_1(1-g)^\alpha)\left(\frac{x}{T}-1\right)\left(1-\frac{x}{K}\right) - c_1 g - m_1 g + m_2(1-g) - (g^\alpha(r_1 g^\alpha + d_1(1-g)^\alpha)\left(\frac{x}{T}\right)\left(1-\frac{x}{K}\right)$$
$$- c_1 g^\alpha + g(1-g)(r_2(1-g)^\alpha + d_2 g^\alpha)\left(\frac{x}{T}\right)\left(1-\frac{x}{K}\right) - c_2 g(1-g))$$

Tumor growth with cytotoxic therapy

$$\dot{x}_1 = x_1(r_1 g^\alpha + d_1(1-g)^\alpha)\left(1-\frac{x}{K}\right) - (c_1+\gamma_1(t))x_1 - m_1 x_1 + m_2 x_2, \tag{3}$$
$$\dot{x}_2 = x_2(r_2(1-g)^\alpha + d_2 g^\alpha)\left(1-\frac{x}{K}\right) - (c_2+\gamma_2(t))x_2 - m_2 x_2 + m_1 x_1. \tag{4}$$

Or seen as:

$$\dot{x} = gx(r_1 g^\alpha + d_1(1-g)^\alpha)\left(1-\frac{x}{K}\right) - (c_1+\gamma_1(t))gx + (x-gx)(r_2(1-g)^\alpha + d_2 g^\alpha)\left(\frac{x}{T}-1\right)\left(1-\frac{x}{K}\right) - (c_2+\gamma_2(t))(x-gx)$$
$$\dot{g} = g(r_1 g^\alpha + d_1(1-g)^\alpha)\left(1-\frac{x}{K}\right) - (c_1+\gamma_1(t))g - m_1 g + m_2(1-g) - (g^\alpha(r_1 g^\alpha + d_1(1-g)^\alpha)\left(\frac{x}{T}\right)\left(1-\frac{x}{K}\right)$$
$$- (c_1+\gamma_1(t))g^\alpha + g(1-g)(r_2(1-g)^\alpha + d_2 g^\alpha)\left(\frac{x}{T}\right)\left(1-\frac{x}{K}\right) - (c_2+\gamma_2(t))g(1-g))$$

Tumor growth with mutation therapy

$$\dot{x}_1 = x_1(r_1 g^\alpha + d_1(1-g)^\alpha)\left(1-\frac{x}{K}\right) - (c_1+\gamma_1(t))x_1 - (m_1+\mu_1(t))x_1 + (m_2+\mu_2(t))x_2, \tag{5}$$
$$\dot{x}_2 = x_2(r_2(1-g)^\alpha + d_2 g^\alpha)\left(1-\frac{x}{K}\right) - (c_2+\gamma_2(t))x_2 - (m_2+\mu_2(t))x_2 + (m_1+\mu_1(t))x_1. \tag{6}$$

Or seen as:

$$\dot{x} = gx(r_1 g^\alpha + d_1(1-g)^\alpha)\left(1-\frac{x}{K}\right) - (c_1+\gamma_1(t))gx + (x-gx)(r_2(1-g)^\alpha + d_2 g^\alpha)\left(\frac{x}{T}-1\right)\left(1-\frac{x}{K}\right) - (c_2+\gamma_2(t))(x-gx)$$
$$\dot{g} = g(r_1 g^\alpha + d_1(1-g)^\alpha)\left(1-\frac{x}{K}\right) - (c_1+\gamma_1(t))g - (m_1+\mu_1(t))g + (m_2+\mu_2(t))(1-g) - (g^\alpha(r_1 g^\alpha + d_1(1-g)^\alpha)\left(\frac{x}{T}\right)\left(1-\frac{x}{K}\right)$$
$$- (c_1+\gamma_1(t))g^\alpha + g(1-g)(r_2(1-g)^\alpha + d_2 g^\alpha)\left(\frac{x}{T}\right)\left(1-\frac{x}{K}\right) - (c_2+\gamma_2(t))g(1-g))$$

These equations show different combinations made in order to carry out some analysis. The first case includes the Allee effect with the parameter T, which occurs when, above a certain threshold, the population size is so tiny that the survival rate or reproductive rate drops because individuals do not reproduce as they do not encounter other individuals from the same population [34]. The other cases ignore it because in the paper [24] they want to showcase the effect of leveraging the coordination game in eliminating the tumor. These models include probability and how the dynamics are structured, which can be seen as a Lotka-Volterra equation [27]. In the second and third cases, the rates of dead cell and mutation are modified and include cytotoxic and mutation therapy, respectively, a value that changes in time. However, the way it varies is not specified.

2.1.2 Model in [25]

This model has one case and includes a function that manages the dynamics as G-function.

$$\dot{x_i} = x_i H_i(\mathbf{u}, \mathbf{x}) = x_i G(v, \mathbf{u}, \mathbf{x})|_{v=u_i}, \tag{7}$$

with the G-function given by the Lotka-Volterra model:

$$G(v, \mathbf{u}, \mathbf{x}) = r - \frac{r}{K(v)} \sum_{j=1}^{n_s} \alpha(v, u_j) x_j. \tag{8}$$

Now,

$$\dot{u_i} = \sigma_i^2 \frac{\partial G(v, \mathbf{u}, \mathbf{x})}{\partial v}|_{v=u_i}. \tag{9}$$

The following distribution function for K and α is:

$$K(v) = k_m exp\left[\frac{-v^2}{2\sigma_k^2}\right] \tag{10}$$

$$\alpha(v, u_j) = 1 + exp\left[\frac{-(v + u_j + \beta)^2}{2\sigma_\alpha^2}\right] - exp\left[\frac{-\beta^2}{2\sigma_\alpha^2}\right] \tag{11}$$

In this case, there is no game theory applied. There is just a G-function that depends on other functions.

2.2 Problem Statement

In this section, we explain the variables and parameters of the problem developed. Here, we take the second case in [24]; however, we present it in a general way, and replicator dynamics is applied to see how the therapy dynamics vary. This problem considers the initial conditions of the two treatment variables and the payoff matrix between them.

To define such problem more formally, let $x_i(t)$ represent the cell cancer population type i, where $i \in \{1, 2\}$, and $\gamma_i(t)$ represent the therapy applied that is added to the cell rates. For this model parameters, K represents the carrying capacity, c_i represent the cell rate death, where $0 \leq c_i \leq 1$; m_i represent the mutation rate, where $0 \leq m_i \leq 1$, and α is the parameter of convexity taken from [24]. Finally, for this model there are two payoff matrices, let $A \in \mathbf{R}^2$ represents the matrix between the two type of cancer cell populations and $B \in \mathbf{R}^2$ represents the matrix between the two therapies. To make it clear, $A_{11} = r_1$ representing the intrinsic growth of the population 1 and $A_{22} = r_2$ representing the intrinsic growth of the population 2, and $A_{12} = d_1$ representing the effect of the population 2 in 1 and $A_{21} = d_2$ representing the effect of population 1 in 2.

3 Proposed Approach

3.1 Model Proposed

The model can be viewed in general terms as follows:

$$\dot{x_i} = x_i \left(r_i \left(\frac{x_i}{\sum_{i=1}^n x_i} \right)^\alpha + d_i \sum_{\substack{j=1 \\ j \neq i}}^n \left(\frac{x_j}{\sum_{i=1}^n x_i} \right)^\alpha \right) \left(\frac{K - \sum_{x=1}^n x_i}{K} \right) - x_i(c_i + m_i + \gamma_i) + \sum_{\substack{j=1 \\ j \neq i}}^n m_j x_j \tag{12}$$

$$\dot{\gamma_i} = \gamma_i \left(F_i(\gamma) - \sum_{j \in S} \gamma_j F_j(\gamma) \right) \tag{13}$$

In this case, we observe a general dynamics of the one seen in [24], but we include a replicator dynamics between the variables γ_1 and γ_2. These variables add to the parameters of the mortality rates and are density-dependent. A clear relationship is seen in this model with the general Lotka-Volterra model [27].

4 Numerical Simulations

In this section, we present three parts. The first part is the sensitivity analysis of the two models of the papers [24] and [25] and the comparison between the models for four cases. This analysis consists on modifying the parameters for both models that are equivalent but not equal. Second, we choose the model that resembles reality and develop a phase diagram analysis.

The third part has four scenarios to illustrate the solution to the problem mentioned. Each scenario has a different initial condition of the therapy γ_i and each scenario evaluates the prisoner's dilemma for the payoffs matrix of the therapy B.

4.1 Sensitivity Analysis

We made comparisons between the models, just considering the percentage of cancer population in both, based on modifications of specific parameters considered equivalent but not equal. The parameters values based are:

Table 1: Table of parameters value model (5) and (6) of [24]

Parameters	Values
K	150
m_1	0.01
m_2	0.01
c_1	0.05
c_2	0.05
r_1	0.4
r_2	0.2
d_1	0
d_2	0
γ_1	0
γ_2	0
μ_1	0
μ_2	0

Table 2: Table of parameters for model [28]

Parameters	Values
r	0.25
k_m	100
σ_k^2	8
σ_α^2	4
β	2
σ_1^2	0
σ_2^2	0.25

For the numerical results we refer to model [24] as model 1 and model [25] as model 2. First, we modify from model 1, K which represented the carrying capacity, and from model 2, k_m which represented the maximum carrying capacity. We show the behavior of the populations when they have the initial constants and compare it by increasing the carrying capacity in each one by its 30% and decreasing it by the same amount (Fig. 2a). Second, we modify r_1 and r_2 of model 1 because they are growth rates of the cancer cells compared to modifying r of model 2 which are the growth rates of all cells. We increase each rate by its 30% and decreasing it by the same amount (Fig. 2b). As shown:

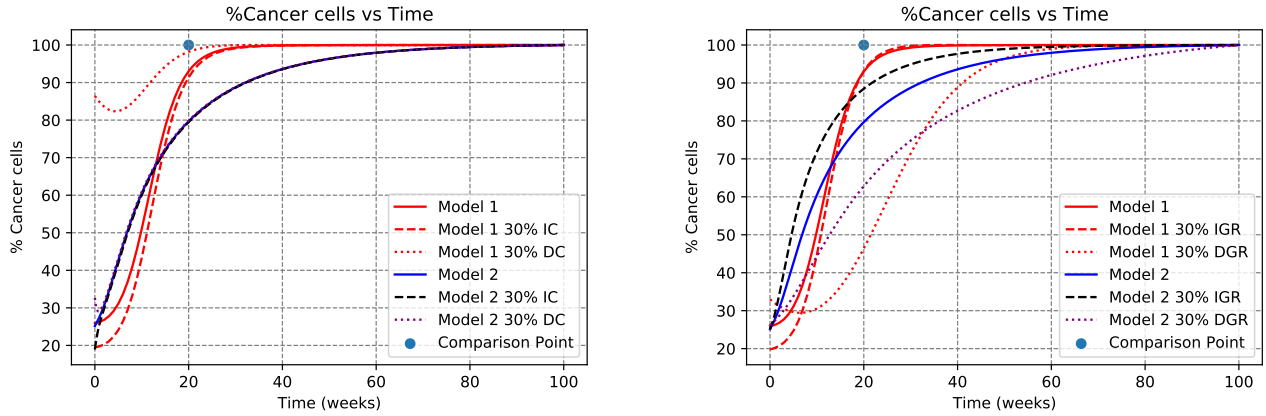

(a) (IC) and (DC)

(b) (IGR) and (DGR)

Figure 2: Increasing and decreasing, carrying capacities 2a and growth rates 2b

In these two cases, we see a comparison of the growth of the models. In Fig. 2a, model 1 shows a relationship between population and the value of K. By increasing the parameter, the population reaches its 100% faster while decreasing it reaches it slower. In comparison with model 2, whose effect by changing k_m is null, since there is no difference and the lines for the cases in the graph overlap. In Fig. 2b, the behavior is similar for both models, increasing the growth rate, the population reaches 100% faster, and decreasing it takes longer.

The third case is when we change the death rates of model 1 of Table 1, which is equivalent to modifying σ_k^2 of model 2. This parameter of the model 2 is a distribution, but the effect is like the cancer cell death rates of the model 1. Increasing these variables has a therapy-like effect, while decreasing them shows the same growth effect as in Fig 2. This case is:

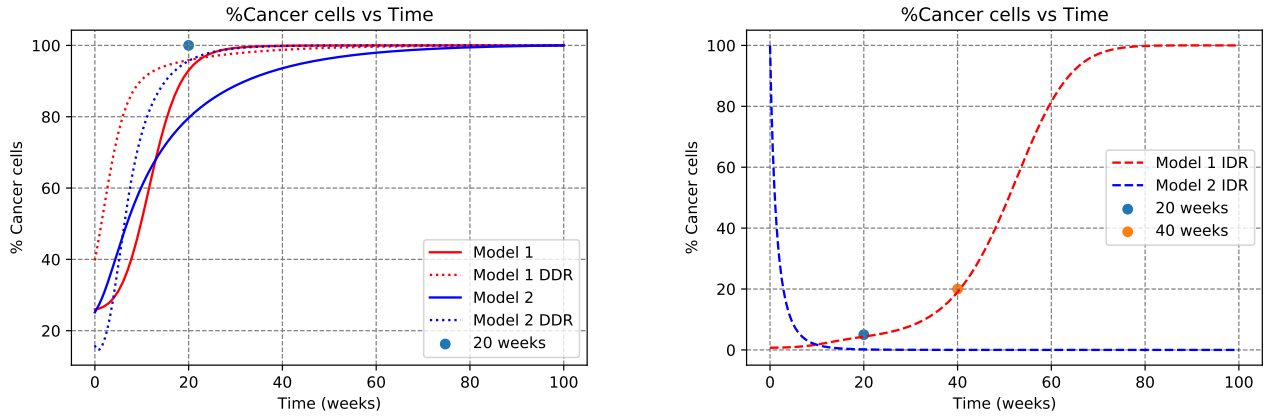

(a) Decreasing death rate (DDR)

(b) Increasing death rate (IDR)

Figure 3: Increasing and decreasing death rate, for model 2, the death rate equivalents the σ_k^2.

In Fig. 3, when the rate of cancer cells decreases and so does the value of σ_k^2, both populations grow faster to their maximum value, as seen in Fig. 3a. As these values decrease respectively, the populations decrease. In the case of model 1, the cancer cell population grew again after 20 weeks. In the other case, it remained close to or had a value of 0 as seen in Fig. 3b.

Finally, the fourth case in this sensitivity analysis is the mutation rates of model 1 versus the change of σ_α^2 of model 2, whose relationship is inversely proportional. We have the following results:

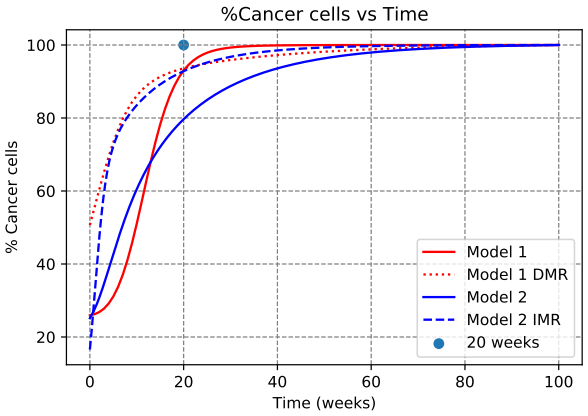

(a) Mutation decreasing model 1 and increasing σ_α^2 model 2

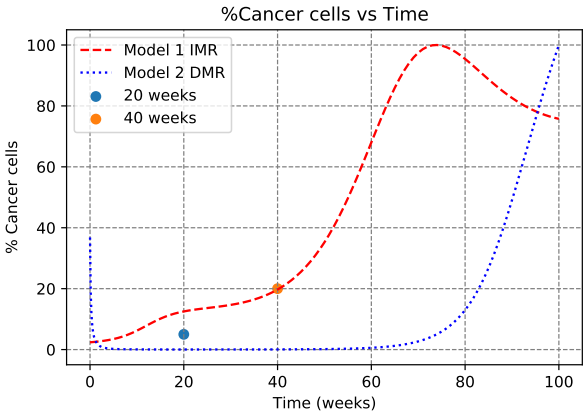

(b) Mutation growth model 1 and decreasing σ_α^2 model 2

Figure 4: Increasing and decreasing mutation rates and σ_α^2.

Fig. 3 shows the inversely proportional relationship. In Fig. 4a, as the mutation rates increase and the value of σ_α^2 decreases, the cancer cell populations grow faster to their maximum. Fig. 4b shows a relevant relationship seen in therapy where both models initially decrease in population size and then grow again.

Now, to determine which is closer to reality, we will specify those points shown in the graphs (comparison points, 20 weeks or 40 weeks) that we use to compare the results data with the literature [35]. The following assumption is made according to different works to determine which model is closer to reality. We consider the size of a particular body site (supposing the ovaries, where tumors form), and according to the reproductive processes mentioned in [1][35], we conclude the following. A cell has an approximate size of $7.5\mu m$[1]; the healthy cell formation lasts approximately 12 hours (depending on the cell varies, we take this value). A cancer cell has no control, therefore is reproduced in double the time as a healthy one. We conclude that in 20 weeks of a person who does not receive treatment, the maximum amount of cancer population is reached. From the analysis also made in the work [35], where the different scenarios of the evolution of a cancer cell are mentioned. For this case we assume a very aggressive cancer. We compare both population percentages at week 20 and calculate the following error for the original case and the cases above, considering the growth:

Table 3: Table of percentage error for growth

Case	Percentage error
Model 1 initial	6.98%
Model 2 initial	20.30%
Model 1 IC	8.52%
Model 2 IC	20.5%
Model 1 DC	5.26%
Model 2 DC	20.07%
Model 1 IGR	6.89%
Model 2 IGR	11.51%
Model 1 DGR	53.61%
Model 2 DGR	37.19%
Model 1 DDR	4.11%
Model 2 D σ_k^2	4.33%
Model 1 DMR	6.40%
Model 2 I σ_α^2	6.63%

In most cases, the percentage error of model 1 is lower than model 2, except for the models with decreasing growth rates.
For cases 3 and 4, where there is cancer therapy, we assume the following according to the literature [35]. The cancer cells usually generate resistance to the therapy [9][11][5][3]. Therefore at the beginning, they are receptive, but they appear again if the therapy is not modified [35]. Works have proven cancer recurrence between 4 and 5 months in cancer patients [10][12]. We assume that there is 5 % of cancer cells at week 20, and at week 40, the growth has quadrupled due to its reproduction rate [1]. Complete extinction of cancer cells cannot be assumed because there is no evidence that therapy can reduce their totality, but doctors keep it under control. The percentage error for these cases of the results are:

Table 4: Table of percentage error for therapy

Case	Percentage error 20 weeks	Percentage error 40 weeks
Model 1 IDR	0.64%	1.00%
Model 2 I σ_k^2	4.83%	19.99%
Model 1 IMR	6.40%	0.29%
Model 2 D σ_α^2	5.12%	20%

From these results, only for the modification case of mutation rate, or σ_α^2 parameter, model 2 has a lower error. Otherwise, it always has a higher error. According to these error results we choose model 1.

4.2 Model Chosen and Phase Diagram Analysis

4.2.1 Model Chosen

In addition to the percentages of the sensitivity analysis, we determine that the [24] model considers many more aspects of cancer, such as death rates and mutation, and also includes competencies such as Lotka-Volterra between both populations. Additionally, model [25] has variables such as evolutionary variables, which are not well described or effectively associated in terms of the biological representation of these variables. The analysis of the model [25] is taking into account cancer cells, and healthy cells, when different authors have mentioned that tumors are composed of different populations of cells [3], which is far from reality. Finally, the model [24] does handle dynamics between the two types of cancer cells population, which, by modifying these dynamics, can be understood as a type of treatment. While in the second model, we need to modify constants in functions that do not allow population management as a game or as competition between them.

4.2.2 Phase Diagram Analysis

To show the cancer cell types' population dynamics, we analyze the model [24].
Tumor growth model in [24]
For this first case, there are parameters involved in limiting growth, how it is growing, and in the population dynamic. These values of the parameters are:

Parameters:

- $K = 100$ Carrying Capacity
- T Allee effect. How it is growing. This value starts in 10.
- m_1 rates (between 0 and 1)
- m_2 rates (between 0 and 1)

- c_1 rates (between 0 and 1)
- c_2 rates (between 0 and 1)

Lastly, there are values that affect the population game:

Values involved in the fitness relation

$$A = \begin{bmatrix} r_1 & d_1 \\ d_2 & r_2 \end{bmatrix}$$

For each of these parameters, we change each one maintaining the other ones with the value used in [24] in order to identify modifications and effects in equilibrium points.
The parameters that were taken as a basis are:

Table 5: Table of parameters

Parameters	Values
K	100
T	10
m_1	0.01
m_2	0.01
c_1	0.05
c_2	0.1
r_1	0.25
r_2	0.17
d_1	0
d_2	0

For the values above and analyzing the phase plane between the two variables g and x, in principle, the phase plane is as follows:

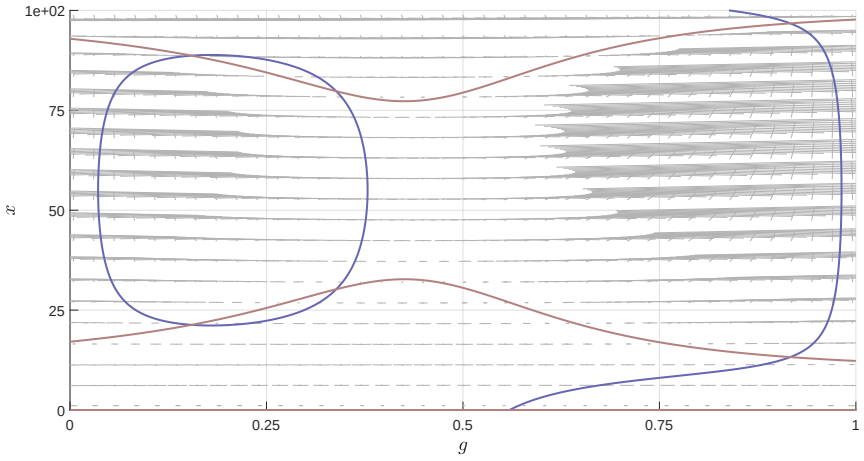

Figure 5: Original dynamics of the model in [24] for relation between g and x.

There are six equilibrium points in this case, but only two are stable. The point when the population of x_1 is small, and x is significant since g represents the composition of x_1, and the point when g is

significant, and x is large. The two stable points will be the two upper corner points in Fig. 5.
For the first constant, we have K, which we modify between 100 and 200. As defined for a carrying capacity, it just limits the capacity of the population. Therefore it just moves upward or downward the nullclines in the phase plane. Because the change is insignificant, we do not present the phase plane. The only effect will be that the maximum value of $x(t)$ will represent this carrying capacity.
The second constant analysis is the Allee effect. This one limits tumor growth. By modifying this variable, we have bifurcations. When $14 \leq T \leq 18$, we go from having six equilibrium points to having four, where we define T as an integer for applying modifications. The two stable equilibrium points are maintained, and the two internal, unstable ones were not from the oval nullcline shown in the phase diagram Fig. 5. However, if we continue to increase the value of T, being $18 < T < 37$, we change from four equilibrium points to two points, besides being a single stable point. This stable point is when the most significant amount of the tumor comes from the population x_1, which is represented on the upper right corner. Finally, if $T \geq 37$, there are zero equilibrium points.
Then, we analyze the proportions of m_1 and m_2. Starting with the first one, we find the following results. When $m_1 \geq 0.06$, we go from having six equilibrium points to having only two. Only one of these points is stable, and it is so when the greatest proportion of the tumor comes from the population x_2, which is represented on the upper left corner in Fig. 5. Furthermore, if m_1 is defined as $0.04 \leq m_1 < 0.06$, then the form of the blue nullclines in the phase diagram is inverted. So there is a change in shape, but there are still two equilibrium points. Therefore, the oval shape would be located on the right side and the arched shape on the left side.
Now, to modify the m_2 variable, we have that if $m_2 \geq 0.02$, then we go from six equilibrium points to two points, where there is only stable; this equilibrium point is on the upper right corner in Fig. 5. Otherwise, the other six points of equilibrium continue the same.
Let's explain the modifications for the constants of c_1 and c_2. For the first one, if $c_1 \leq 0.03$, we go from six equilibrium points to two, where x_1 is predominant. Between these two points the stable one is in the upper right corner in Fig. 5. Then if $c_1 > 0.10$, it changes from six equilibrium points to four equilibrium points. The phase diagram maintains the two stable equilibrium points; the oval figure interchanges positions with the arched figure of the nullclines. The location of the lost equilibrium points is on the right side of the oval shape's interiors. Finally, if $c_1 \geq 0.42$ then just x_2 is predominant and it is the unique stable equilibrium point.
For the c_2, we have three changes. The first change is when $c_2 \leq 0.01$ goes from having six equilibrium points to having two. Here we still have the switching of the blue nullclines, the oval figure on the right side, and the arched figure on the left. The two equilibrium points allude to the arched part on the left, where only one is stable when x_2 dominates; this one is on the upper left corner. The second change is when $0.2 < c_2 < 0.22$ has four equilibrium points, but x_1 is still predominant because it is the only one stable. The phase diagram figure have the blue nullclines located as in the original form. However, only the two equilibrium points of the arched shape are maintained. For this variable, the last possibility is if $c_2 \geq 0.22$ and with this value, it is guaranteed that only two equilibrium points exist and only the population x_1 prevails to compose x.

Tumor growth with cytotoxic therapy

In this case, the values of the parameters change in general, but the same effect mentioned above still exists. The parameters used for this and the following model are:

Table 6: Table of parameters

Parameters	Values
K	150
m_1	0.01
m_2	0.01
c_1	0.05
c_2	0.05
r_1	0.4
r_2	0.2
d_1	0
d_2	0
γ_1	0.4
γ_2	0

Analyzing this case, the effects of the variables increase $\gamma's$ whose values influence cell mortality rates. The effect, in general, moves the nullcline. However, there is only one equilibrium point, and since, in this case, x_2 is resistant while x_1 is sensitive to treatment, then it only makes the population to stay at x_2.

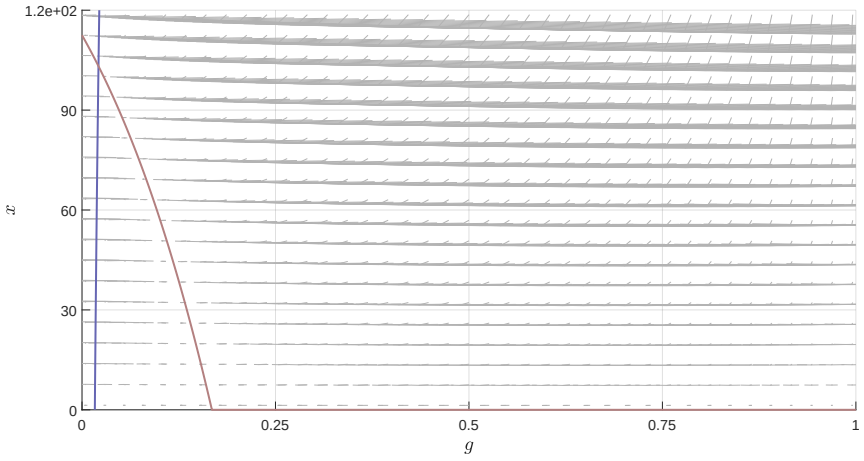

Figure 6: Phase diagram of x vs g with original therapy.

Tumor growth with mutation therapy
The parameters used in this case are:

Table 7: Table parameters

Parameters	Values
K	150
m_1	0.01
m_2	0.01
c_1	0.05
c_2	0.05
r_1	0.4
r_2	0.2
d_1	0
d_2	0
γ_1	0
γ_2	0
μ_1	0
μ_2	0.01

The analysis, in this case, is very similar to the first analysis in case 1. However, the only difference is that if the cell mortality rates are not modified and only the mutation rates are, this modifies the equilibrium points. It is generating bifurcations, changing equilibrium points, and generating treatments. Through the analysis above, it is verified how the dynamics are affected by each variable. Thus, in making our model, we will use the initial parameters values to ensure two stable equilibrium points.

4.3 Proposed scenarios for the problem

For this problem, we propose using a matrix B, the payment matrix, as a prisoner's dilemma between the therapy variables.

$$A = \begin{bmatrix} 3 & 1 \\ 4 & 2 \end{bmatrix}$$

We maintain the initial conditions of x_1 and x_2. In addition, all variables involved in the problem have the same values, as shown in the following table. The only thing that changes among scenarios is the initial conditions of the therapies.

Table 8: Table of parameters

Parameters	Values
K	150
m_1	0.01
m_2	0.01
c_1	0.05
c_2	0.05

Initial conditions are:

- $x_1 = 50$
- $x_2 = 70$

4.3.1 First scenario:

Initial conditions for therapy are:

- $\gamma_1 = 0.1$
- $\gamma_2 = 0.5$

4.3.2 Second scenario:

Initial conditions for therapy are:

- $\gamma_1 = 0.1$
- $\gamma_2 = 0.9$

4.3.3 Third scenario:

Initial conditions for therapy are:

- $\gamma_1 = 0.4$
- $\gamma_2 = 0$

4.3.4 Fourth scenario:

Initial conditions for therapy are:

- $\gamma_1 = 0.9$
- $\gamma_2 = 0$

For comparison with the literature, we use these initial conditions for the model [24] with constant cytotoxic therapies. The simulations are:

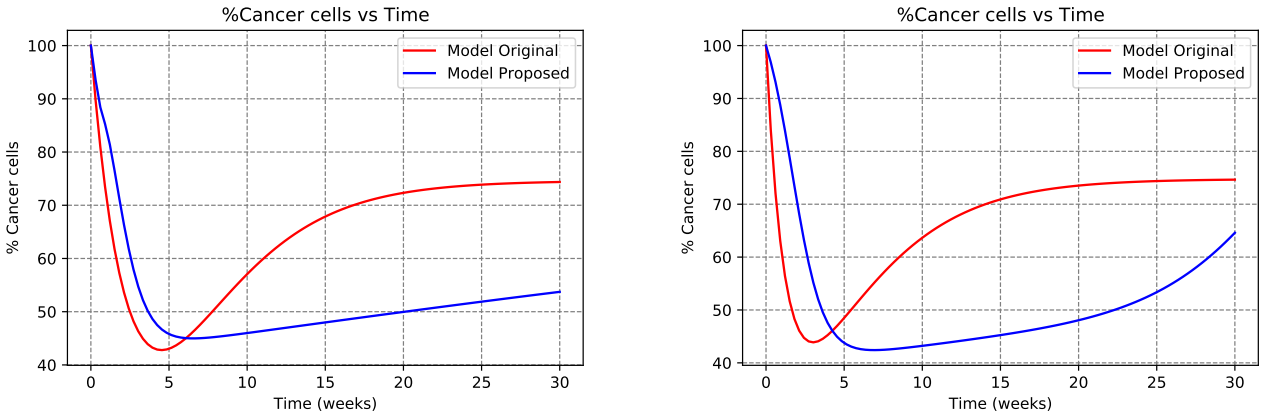

(a) Scenario 1

(b) . Scenario 2

Figure 7: Relationship between % population and time for scenario 1 and 2.

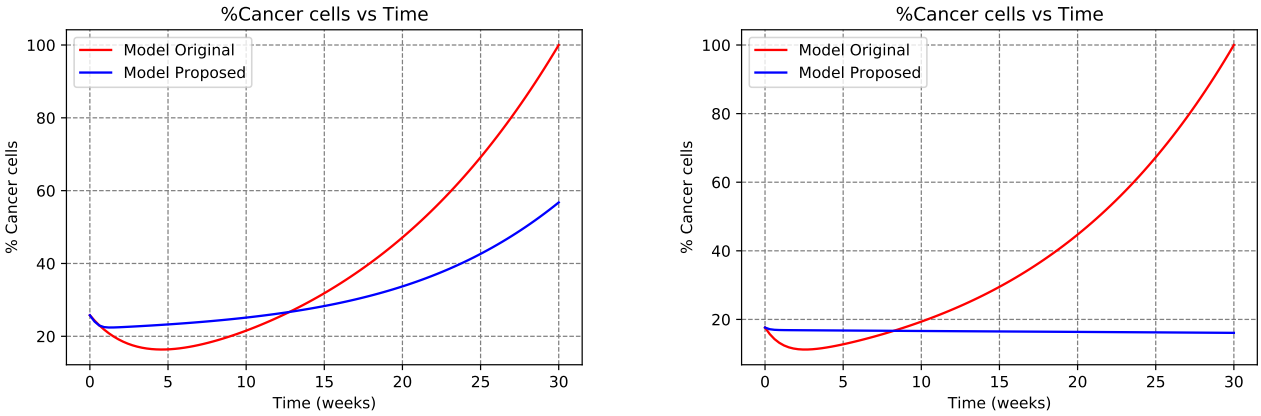

(a) . Scenario 3

(b) Scenario 4

Figure 8: Relationship between % population and time for different scenarios 3 and 4.

We randomly choose the four scenarios above to expose different outcomes to an applied treatment. We review the final percentage of the cancer population after the applied therapy, and the lower one shows better management of cytotoxic therapy. The percentage amount were:

Table 9: Percentage of cancer cells for each scenario.

Case	Scenario 1	Scenario 2	Scenario 3	Scenario 4
Original Model	74.37%	74.65%	100.00%	100.00%
Model Proposed	53.73%	64.60%	56.76%	16.08%

From these results, we can comment that by applying a replicator dynamics, we are able to visualize that we cause a change in the treatment effect. Also, the effect of the therapy on the population dynamics varies depending on the initial conditions. In scenarios 3 and 4, we take into account that population x_2 is resistant and therefore when applying a lower therapy to x_1 initially as in scenario 3, while applying a higher therapy as in scenario 4, we observe whether the tumor remains the same or decreased in size. In this way, we interpret these effective dynamics for chemotherapy and thus understand how to apply the different treatments at what times to realize a population decrease. The percentages in each scenario of the proposed model are lower compared to the original model at the end of 30 weeks.

5 Conclusions and future works

In this paper, we have demonstrated a comparison between two models obtained from literature. We have performed a sensitivity analysis to determine what effects certain constants generated in these dynamics. We have identified which of the two models most closely resembled reality. We have modified the game-based model with different payoff matrices to model different matrix games. We have made a variation to the therapies by linking it with replicator dynamics. We have been able to show a therapy that depends on densities and changes over time. Also, we have linked this therapy to its initial conditions. Future work should develop a way to evaluate whether this type of therapy resembles reality in addition to being able to analyze the points of equilibrium in this model where we include these therapy dynamics. Also, it should include more factors in the model that benefits or affect a cancer cell, e.g, pH and environment.

References

[1] R. A. Weinberg, *The biology of cancer*. Garland Science, 2007.

[2] P. J. Campbell and GBD-Collaborators, "Pan-cancer analysis of whole genomes," *Nature*, vol. 578, pp. 82–93, Feb 2020.

[3] P. M. Enriquez-Navas and R. A. Gatenby, "28 - evolutionary strategies to overcome cancer cell resistance to treatment," in *Phenotypic Switching* (H. Levine, M. K. Jolly, P. Kulkarni, and V. Nanjundiah, eds.), pp. 691–703, Academic Press, 2020.

[4] J.-P. Capp, "Cancer stem cells: From historical roots to a new perspective," *Journal of Oncology*, vol. 2019, p. 5189232, Jun 2019.

[5] A. Dujon, A. Aktipis, C. Alix-Panabières, S. Amend, A. Boddy, J. Brown, J.-P. Capp, J. DeGregori, P. Ewald, R. Gatenby, F. Thomas, and B. Ujvari, "Identifying key questions in the ecology and evolution of cancer," *Evolutionary Applications*, vol. 14, pp. 877–892, 2021.

[6] R. A. Beckman, I. Kareva, and F. R. Adler, "How should cancer models be constructed?," *Cancer Control*, vol. 27, no. 1, p. 1073274820962008, 2020.

[7] S. Park, A. Bizyaeva, M. Kawakatsu, A. Franci, and N. E. Leonard, "Tuning cooperative behavior in games with nonlinear opinion dynamics," 2021.

[8] A. Oroji, M. Omar, and S. Yarahmadian, "An îto stochastic differential equations model for the dynamics of the mcf-7 breast cancer cell line treated by radiotherapy," *Journal of Theoretical Biology*, vol. 407, pp. 128–137, 2016.

[9] J. West, Y. Ma, and P. K. Newton, "Capitalizing on competition: An evolutionary model of competitive release in metastatic castration resistant prostate cancer treatment," *Journal of Theoretical Biology*, vol. 455, pp. 249–260, 2018.

[10] J. J. Cunningham, J. S. Brown, R. A. Gatenby, and K. Staňková, "Optimal control to develop therapeutic strategies for metastatic castrate resistant prostate cancer," *Journal of Theoretical Biology*, vol. 459, pp. 67–78, 2018.

[11] J. Salimi Sartakhti, M. H. Manshaei, and M. Sadeghi, "Mmp–timp interactions in cancer invasion: An evolutionary game-theoretical framework," *Journal of Theoretical Biology*, vol. 412, pp. 17–26, 2017.

[12] L. You, J. S. Brown, F. Thuijsman, J. J. Cunningham, R. A. Gatenby, J. Zhang, and K. Staňková, "Spatial vs. non-spatial eco-evolutionary dynamics in a tumor growth model," *Journal of Theoretical Biology*, vol. 435, pp. 78–97, 2017.

[13] N. Laleh, C. Loeffler, J. Grajek, K. Staňková, A. Pearson, H. Muti, C. Trautwein, H. Enderling, J. Poleszczuk, and J. Kather, "Classical mathematical models for prediction of response to chemotherapy and immunotherapy," *PLoS Computational Biology*, vol. 18, no. 2, 2022.

[14] D. A. Deenen, B. Maljaars, L. C. Sebeke, B. de Jager, E. Heijman, H. Grüll, and W. P. M. H. Heemels, "Offset-free model predictive temperature control for ultrasound-based hyperthermia cancer treatments," *IEEE Transactions on Control Systems Technology*, vol. 29, no. 6, pp. 2351–2365, 2021.

[15] H. Khadem, H. Kebriaei, and Z. Veisi, "Inactivation of tumor suppressor genes and cancer therapy: An evolutionary game theory approach," *Mathematical Biosciences*, vol. 288, pp. 84–93, 2017.

[16] B. Wölfl, H. te Rietmole, M. Salvioli, A. Kaznatcheev, F. Thuijsman, J. Brown, B. Burgering, and K. Staňková, "The contribution of evolutionary game theory to understanding and treating cancer," *Dynamic Games and Applications*, 2021.

[17] I. Kareva, "Prisoner's dilemma in cancer metabolism," *PLOS ONE*, vol. 6, pp. 1–9, 12 2011.

[18] J. J. Cunningham, R. A. Gatenby, and J. S. Brown, "Evolutionary dynamics in cancer therapy," *Molecular Pharmaceutics*, vol. 8, pp. 2094–2100, Aug. 2011.

[19] J. S. Brown, "Why darwin would have loved evolutionary game theory," *Proceedings of the Royal Society B: Biological Sciences*, vol. 283, Sept. 2016.

[20] J. West, Z. Hasnain, J. Mason, and P. K. Newton, "The prisoner's dilemma as a cancer model," *Convergent Science Physical Oncology*, vol. 2, July 2016.

[21] R. Axelrod, D. E. Axelrod, and K. J. Pienta, "Evolution of cooperation among tumor cells," *Proceedings of the National Academy of Sciences*, vol. 103, no. 36, pp. 13474–13479, 2006.

[22] M. Archetti and K. J. Pienta, "Cooperation among cancer cells: applying game theory to cancer," *Nature Reviews Cancer*, vol. 19, pp. 110–117, Feb. 2019.

[23] I. P. Tomlinson, "Game-theory models of interactions between tumour cells," *European Journal of Cancer*, vol. 33, pp. 1495–1500, Aug. 1997.

[24] P. Bayer, R. Gatenby, P. McDonald, D. Duckett, K. Staňková, and J. Brown, "Coordination games in cancer," *PLoS ONE*, vol. 17, 2022.

[25] T. L. Vincent and J. S. Brown, *Evolutionary Game Theory, Natural Selection, and Darwinian Dynamics*. Cambridge University Press, 2005.

[26] S. Park, N. Martins, and J. Shamma, "From population games to payoff dynamics models: A passivity-based approach," vol. Proceedings of the 2019 IEEE Conference on Decision and Control - December, pp. 6584–6601, 2019.

[27] W. H. Sandholm, *Population games and evolutionary dynamics*. Economic learning and social evolution, MIT Press, 2010.

[28] J. Hofbauer and K. Sigmund, *Evolutionary Games and Population Dynamics*. Cambridge University Press, 1998.

[29] V. Křivan, T. E. Galanthay, and R. Cressman, "Beyond replicator dynamics: From frequency to density dependent models of evolutionary games," *Journal of Theoretical Biology*, vol. 455, pp. 232–248, 2018.

[30] G. J. Kimmel, P. Gerlee, J. S. Brown, and P. M. Altrock, "Neighborhood size-effects shape growing population dynamics in evolutionary public goods games," *Communications Biology*, vol. 2, p. 53, Feb 2019.

[31] R. A. Gatenby and T. L. Vincent, "Application of quantitative models from population biology and evolutionary game theory to tumor therapeutic strategies," *Mol Cancer Ther*, vol. 2, pp. 919–927, Sept. 2003.

[32] P. D. Taylor and L. B. Jonker, "Evolutionarily stable strategies and game dynamics," *Bellman Prize in Mathematical Biosciences*, vol. 40, pp. 145–156, 1978.

[33] I. Samokhin, T. Yakushkina, D. Markin, and A. S. Bratus, "Fitness landscape adaptation in open replicator systems with competition: application to cancer therapy," 2021.

[34] E. Angulo, G. W. Roemer, L. Berec, J. Gascoigne, and F. Courchamp, "Double allee effects and extinction in the island fox," *Conserv Biol*, vol. 21, pp. 1082–1091, Aug. 2007.

[35] M. A. Smith, C. B. Nielsen, F. C. Chan, A. McPherson, A. Roth, H. Farahani, D. Machev, A. Steif, and S. P. Shah, "E-scape: interactive visualization of single-cell phylogenetics and cancer evolution," *Nature Methods*, vol. 14, pp. 549–550, Jun 2017.